AJNR

Toward a Better Understanding of Brain Lesions during Metachromatic Leukodystrophy Evolution

A. Martin, C. Sevin, C. Lazarus, C. Bellesme, P. Aubourg and C. Adamsbaum

AJNR Am J Neuroradiol 2012, 33 (9) 1731-1739
doi: https://doi.org/10.3174/ajnr.A3038
http://www.ajnr.org/content/33/9/1731

ORIGINAL RESEARCH

Toward a Better Understanding of Brain Lesions during Metachromatic Leukodystrophy Evolution

A. Martin
C. Sevin
C. Lazarus
C. Bellesme
P. Aubourg
C. Adamsbaum

BACKGROUND AND PURPOSE: The prospect of new therapies in MLD stresses the need to refine the indications for treatment. The aim of this study was, therefore, to perform a detailed analysis of MRI brain lesions at diagnosis and follow-up, to better understand the natural history of MLD.

MATERIAL AND METHODS: This retrospective case-control study (2005–2010) looked at 13 patients with MLD (2–5 years of age) with 28 MRIs (mean follow-up, 2 years), compared with 39 age- and sex-matched controls. All MRIs were evaluated qualitatively and semiquantitatively. The Student *t* test, Wilcoxon signed rank test, and Pearson correlation were used for statistical analysis ($P < .05$).

RESULTS: In addition to diffuse symmetric supratentorial WM T2 hyperintensities with a tigroid pattern (70%) and T2 hyperintensities in the CC (100%) and internal capsules (46%), we found significant GM abnormalities such as thalamic T2 hypointensity (92%), thalamic (23%, $P < .05$, EJ) and caudate nuclei (23%, $P < .05$, EJ) atrophy, and cerebellar atrophy without WM involvement (15%). The pattern of splenium involvement progression was misleading, with initially diffuse high signal intensity, which later became curvilinear before finally progressing to atrophy (23%, $P < .05$; EJ). This should not be mistaken for a disease regression. Spectroscopy confirmed a decrease in the NAA/Cr ratio, an increase in the Cho/Cr ratio and in myo-inositol, and a lactate resonance.

CONCLUSIONS: Thalamic changes may be a common finding in MLD, raising the prospect of primary GM lesions. This may prove important when evaluating the efficacy of new treatments.

ABBREVIATIONS: ARSA = arylsulfatase A; CC = corpus callosum; CT = capsulothalamic; GM = gray matter; EJ = early juvenile form; LI = late infantile form; MLD = metachromatic leukodystrophy

MLD is an autosomal recessive lysosomal storage disorder more often due to a deficiency in the enzyme ARSA than to a Saposin B deficiency. The resulting inability to break down sulfatides leads to central and peripheral demyelination.[1] Three clinical subtypes based on the age of onset are well-recognized and are helpful, but those probably represent a continuum related, in part, to the actual magnitude of enzyme deficiency/residual enzyme activity, rather than truly different diseases. In order of frequency, the subtypes are the LI (60%), the juvenile form (which is further divided into an early onset before 6 years and later onset after 6 years) (20%–30%), and the adult form (10%–20%).[2] Classically, MRI shows bilateral symmetric involvement of the periventricular WM, CC, corticospinal tracts, and WM of the cerebellum.[1,3] While the prospect of new therapies, like the gene therapy used in other leukodystrophies,[4] has elicited a severity scoring system[5] to refine the indications for treatment, the course of MLD remains poorly understood. In particular, there has been little study of the GM involvement suggested in the literature.[6] Indeed, in the MLD mouse model as in patients, sulfatide storage occurs mainly in glial cells but also in neurons.[7,8]

The aim of this study was, therefore, to perform a detailed qualitative and semiquantitative analysis of MRI brain lesions in patients with MLD at diagnosis and follow-up, to better understand the natural history of the disease.

Materials and Methods

Patients

This was a single-center retrospective case-control study conducted between 2005 and 2010 at a leukodystrophy referral center. Thirteen untreated children were included, by using the following eligibility criteria: laboratory diagnosis of MLD; decreased level of ARSA in leukocytes, increased level of sulfatides in the urine, and presence of *ARSA* gene mutation; at least 1 brain MRI including, at a minimum, T1-weighted, T2-weighted, and FLAIR sequences in 2 imaging planes.

The patients were classified as either LI or EJ, defined clinically by age of onset of symptoms (ie, younger than 2 years for LI, and younger than 6 years for EJ).

The control population was represented by 39 brain MRIs, obtained between 2005 and 2010 on 7 girls (18%) and 32 boys (82%), 1 year 3 months to 6 years of age, for growth or minor language delay, by using the same imaging parameters as those used for the patients with MLD, and interpreted as having normal findings by a senior radiologist experienced in pediatric radiology (C.A.). The 39 controls were age- and sex-matched to the patients.

Image Acquisition

All of the MRI was performed on a 1.5T system (Signa; GE Healthcare, Milwaukee, Wisconsin or Avanto; Siemens, Erlangen, Germany) by using a standardized protocol for leukodystrophies that included a sagittal T1 (300–500/5–13 ms [TR/TE]), axial T2 (2300–5270/87–

Received November 18, 2011; accepted after revision January 4, 2012.

From AP-HP, Bicêtre Hospital, Pediatric Radiology Department (A.M., C.A.), and Neuropediatrics Department (C.S., C.B., P.A.), Le Kremlin Bicêtre, France; AP-HP, Cochin-Broca-Hôtel Dieu Hospital, Unit of Epidemiology and Biostatistics (C.L.), Paris, France; and Paris Descartes University, Faculty of Medecine (C.A., C.L., P.A.), Paris, France.

Please address correspondence to Catherine Adamsbaum, MD, Service de Radiologie Pédiatrique, CHU Bicêtre, 78 rue du Général-Leclerc, 94275 Le Kremlin-Bicêtre, France; e-mail: adamsbaum.catherine@gmail.com

Indicates article with supplemental on-line tables.

Indicates article with supplemental on-line figures.

http://dx.doi.org/10.3174/ajnr.A3038

142 ms [TR/TE]), and axial FLAIR (8000–10,000/94–153/2000–2500 ms [TR/TE/TI]) sequence. The maximum section thickness was 5 mm. The DWI was acquired in the anterior/posterior commissure plane by using 2 different b-values ($b = 0$ and $b = 1000$ s/mm^2). ADC maps were created automatically (Avanto, Siemens) or with dedicated software (FuncTool, GE Healthcare). Single-voxel spectroscopy sequences were performed following the MRI protocol by using a point-resolved spectroscopy sequence with short and long TEs (35 and 144 ms, respectively) by the single-voxel technique. The size of the VOI located in the abnormal juxtaventricular WM was $2 \times 1.5 \times 1.5$ cm^3.

Image Analysis

All MRI was analyzed jointly by a senior (C.A.) and junior (A.M.) radiologist, by using the reading protocol below (On-line Figs 1–4).

Changes in supratentorial WM signal intensity and volume were evaluated and classified according to their extent and topography: periventricular (frontal, temporal, and parieto-occipital), semiovale center, internal capsule, corticospinal tracts, CC, and subcortical U fibers. "Tigroid " appearance, defined as small scattered areas of normal WM signal intensity within the demyelinated WM, was marked as present or absent. CC atrophy was evaluated on the midsagittal T1-weighted image by measuring the thickness at the genu, the body, and the splenium by using the methods of Barkovich and Kjos[9] and Rakic and Yakovlev.[10] Cerebral atrophy was evaluated on the axial T2-weighted sequences by transverse measurement of the frontal horns and central portions of the lateral ventricles and of the third ventricle.

Cerebellar WM signal-intensity changes were noticed and the atrophy of the vermis was evaluated according to the size of the fourth ventricle and the primary fissure, visible or enlarged on the midsagittal T1-weighted image. Because coronal sections were not systematically available, the volume of the cerebellar hemispheres was not evaluated.

Signal-intensity and size changes (diameters, perimeter, and area) of the thalami, caudate, and lenticular nuclei were analyzed. The direction of progression of signal-intensity changes and their modifications in signal intensity and volume were analyzed in follow-up MRI in 8 patients (5 LI and 3 EJ).

On DWI, several regions of interest were placed on the $b = 0$ images (CC, splenium, and genu; abnormal frontal and occipital WM in contact with the ventricle; thalami, and caudate and lenticular nuclei) and transferred to the ADC map. The ADC values (in square millimeters per second) were compared with the data in the literature[11] because of the lack of DWI in controls.

Each MRI was scored according to the scoring system of Eichler et al,[5] and correlations with the different variables were analyzed.

Statistical Analysis

Statistical analysis was performed by using SAS 9.1 for Windows (SAS, Cary, North Carolina). A Student *t* test was used for comparing means, after checking for normal distribution and equal variances (histogram and Shapiro-Wilk test). In cases in which variances were not equal, we used the Wilcoxon signed rank test. A Pearson correlation was used to study correlation. A $P < .05$ was considered statistically significant.

Results

Patients

In all, 28 MRIs were analyzed in 13 children with MLD, ranging in age from 2 years 1 month to 5 years 5 months at initial MRI. There were 10 with LI (9 boys and 1 girl; mean age, 2 years 6 months at initial MRI; mean interval between onset of symptoms and initial MRI of 1 year 2 months) (On-line Table 1). The mean length of clinical follow-up for LI patients was 1 year (range, 9–17 months), with a mean inter-MRI interval of 6 months (range, 3–12 months). There were 3 with EJ (3 girls; mean age, 5 years at initial MRI; mean interval between onset of symptoms and initial MRI of 1 year 1 month) (On-line Table 2). The mean length of clinical follow-up for EJ patients was 2 years 9 months (range, 12–65 months), with a mean inter-MRI interval of 1 year 4 months (range, 6–125 months).

Initial MRI

All patients (10/10 LI, 3/3 EJ) exhibited typical initial lesions, with bilateral symmetric confluent hyperintensities in the supratentorial periventricular WM on the T2-weighted images. There was extensive frontal, parietal, and occipital involvement in 7/10 LI patients (mean duration of disease, 1 year 3 months) and 3/3 EJ patients (mean duration of disease, 1 year 1 month) and semiovale center involvement in 6/10 LI patients (mean duration of disease, 1 year 4 months) and 3/3 EJ patients. A tigroid pattern was seen in 6/10 LI patients (mean duration of disease, 1 year 4 months) and all 3 of the EJ patients, all scoring >13 (Fig 1). There was no involvement of the subcortical U fibers.

Concerning the degree of T2 hyperintensity, graded according to the scoring system of Eichler et al[5] (faint or attenuated), all patients with an initial extensive frontal, parietal, and occipital involvement had an attenuated T2 hyperintensity. All patients had predominantly occipital involvement, and frontal involvement was barely visible initially in 4/10 LI patients (faint T2 hyperintensity).

A hyperintense signal intensity in the posterior limb of the internal capsule extending into the corticospinal tracts of the brain stem was present in 4/10 LI and 2/3 EJ patients on their initial T2-weighted images, all with MRI scores of >19 (Fig 2).

Follow-Up

The MRI severity score was calculated for all initial and follow-up MRI. Eight patients (5/10 LI and 3/3 EJ) had ≥1 follow-up MRI as their disease progressed. For the 5 LI patients with follow-up MRI, the mean initial score was 8.8 and the mean follow-up score was 15.5 (mean follow-up interval, 1 year). For the 3 EJ patients with follow-up MRI, the mean initial score was 22 and the mean follow-up score was 23.7 (mean follow-up interval, 2 years 8 months) (Fig 3).

Lesion changes occurred with time only in the LI patients: All showed an increase in T2 signal intensity (5/5 LI; mean duration of disease, 1 year 8 months), and all showed occipitofrontal progression. Extension of abnormal WM signal intensity to the semiovale centers occurred at a mean age of 3 years 2 months (mean duration of disease, 1 year 9 months) in 4/5 LI patients who had initially no abnormal signal intensity in the semiovale centers. Two LI patients (2/5) developed a tigroid appearance in their WM at a mean age of 3 years 2 months (mean duration of disease, 1 year 11 months).

Particular Structure Involvements

CC. CC involvement was initially present in all patients (13/13) as evidenced by abnormally high T2 signal intensity.

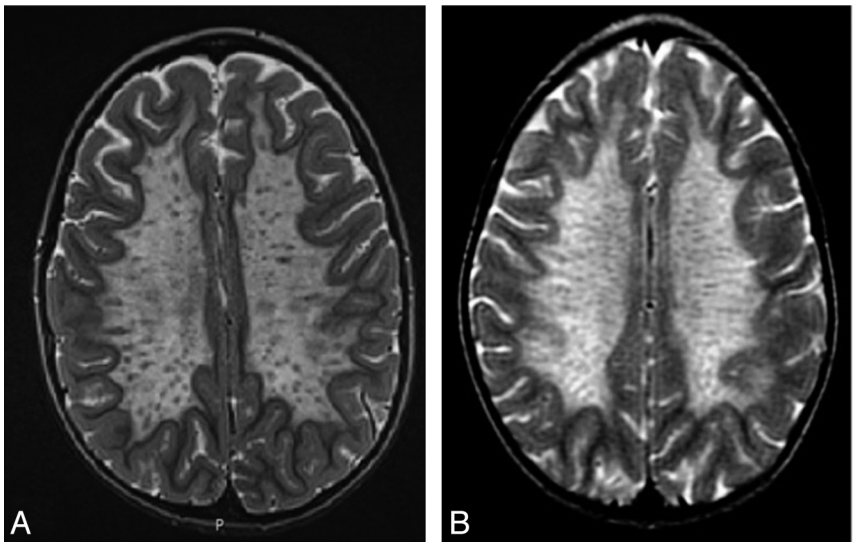

Fig 1. *A*, EJ diagnosed at the age of 4 years 6 months. MRI performed at the age of 10 years, 10 months. *B*, LI, 2 years, 9 months. Note the tigroid appearance of the WM on T2-weighted sequences.

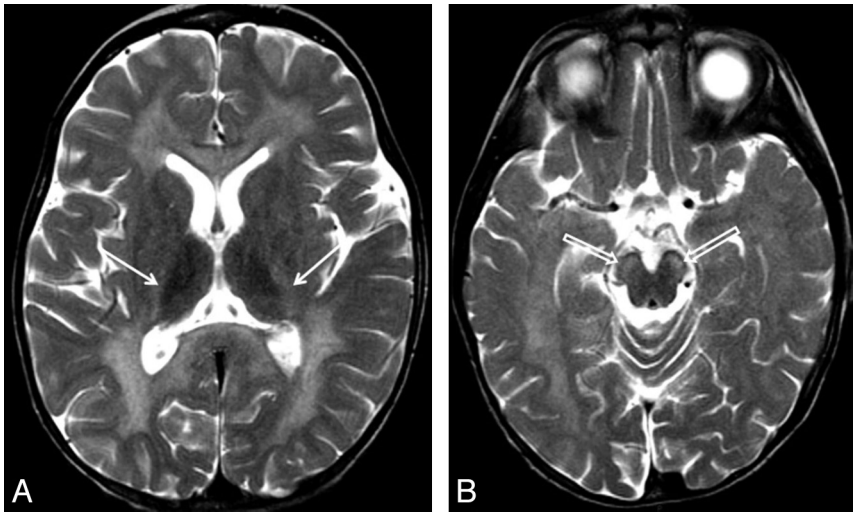

Fig 2. LI, 2 years 7 months. *A*, Involvement of the posterior limb of the internal capsules (*solid arrows*). *B*, Involvement of the corticospinal tracts in the brain stem (*open arrows*) on axial T2-weighted sequences.

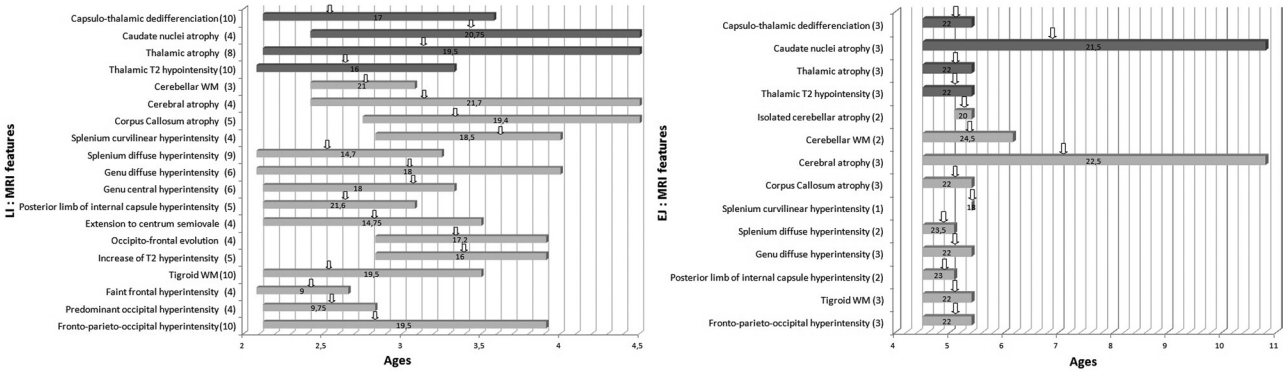

Fig 3. MRI manifestations in LI and EJ patients (number of patients with each abnormality in parentheses) as a function of age of onset. Dark gray bars indicate GM abnormalities; light gray bars, WM abnormalities. Arrows indicate the mean age for each category. The mean score is noted at the center of each bar.

In the axial plane, we observed several patterns of lesions: a diffuse lesion (9/13 patients) in the splenium (4/10 LI) or in both the genu and splenium (3/10 LI, 2/3 EJ); a central lesion in the genu (2/10 LI); or a curvilinear lesion in the splenium (1/10 LI and 1/3 EJ patients) (Fig 4). CC changes were observed in 4/5 LI patients with follow-up: In 3/5 LI patients, a

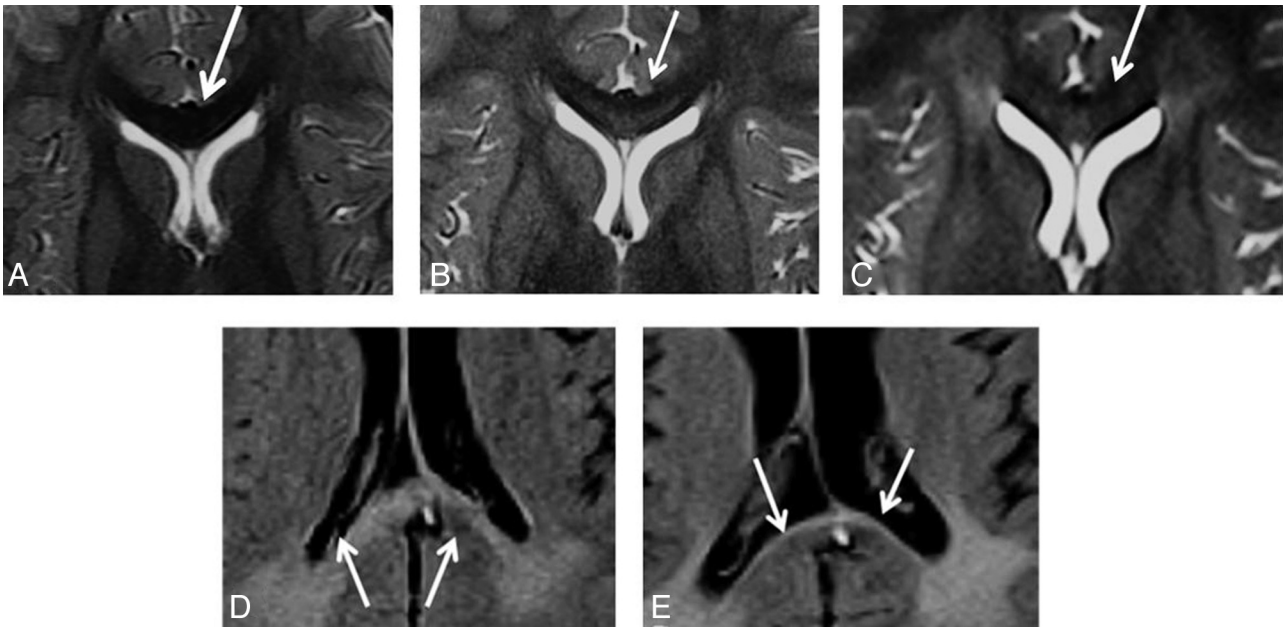

Fig 4. LI. Axial T2-weighted sequence, genu of CC (*arrows*). *A*, Normal (3 years 1 month). *B*, Central involvement (3 years 4 months). *C*, Diffuse involvement (4 years). EJ. Axial FLAIR sequence, splenium of the CC (*arrows*). *D*, Diffuse hyperintensity (3 years 6 months), then curvilinear hyperintensity (4 years 6 months) (*E*).

Table 1: Mean values of CC thicknesses (EJ) compared with controls at the same age, with corresponding *P* values

	Values (mean ± SE) (mm)		
Localization	EJ	Controls	*P* Value
Genu of CC	7.6 ± 1	9.9 ± 0.4	.13
Mild body of CC	3.5 ± 0,4	5.8 ± 0.2	.33
Splenium of CC	6 ± 0.7	8.3 ± 0.2	<.05

Note:—SE indicates standard error.

diffuse lesion of the splenium (mean MRI score, 9; mean age, 2 years 6 months; mean duration of disease, 1 year 6 months) transformed into a curvilinear pattern (mean MRI score, 17; mean age, 3 years 10 months; mean duration of disease, 2 years, 6 months) (Fig 4). In 4/5 LI patients with an initial normal genu, a central lesion appeared (mean MRI score, 17; mean age, 3 years 4 months; mean duration of disease, 2 years 3 months) and then transformed in 2 patients with longer follow-up into a diffuse lesion (mean MRI score, 17; mean age, 3 years 11 months; mean duration of disease, 2 years, 6 months) (Fig 4). In the LI patients, the mean CC thinning was not significant at the first MRI. For the 3/3 EJ patients, the mean CC thinning was 39% for the body and 27% for the splenium at the initial MRI (mean age, 5 years; mean duration of disease, 1 year 1 month) with no CC changes during the course of follow-up. The difference with normal values for age was statistically significant ($P < .05$) for the splenium (Table 1). CC atrophy was associated with cerebral atrophy in only 1/3 patients with EJ.

Brain Volume. Cerebral atrophy was initially present in 4/10 LI (mean age, 2 years 8 months; mean duration of disease, 1 year 3 months) and in 1/3 EJ patients (age, 4 years 6 months; duration of disease, 8 months). In LI patients, it manifested as a 46% enlargement in the frontal horns and an 18% enlargement in the occipital horns compared with the controls. In EJ patients, the frontal horns were enlarged by 54% and the occipital horns, by 10% relative to the controls. These differences

Table 2: Mean values of measures of frontal and occipital horns and third ventricle compared with controls at the same age, with corresponding *P* values (LI)

	Values (mean ± SE) (mm)		
Measures	LI	Controls	*P* Value
R frontal horn	5.4 ± 0.8	3.7 ± 0.2	<.0001
L frontal horn	5.4 ± 0.8	3.7 ± 0.2	<.0001
R occipital horn	8.5 ± 0.8	7 ± 0.3	<.0001
L occipital horn	8.5 ± 0.7	7.4 ± 0.3	<.0001
Third ventricle	6 ± 0.6	4.2 ± 0.3	<.0001

Note:—R indicates right; L, left.

Table 3: Mean values of measures of frontal and occipital horns and third ventricle, compared with controls at the same age, with corresponding *P* values (EJ)

Measures	EJ	Controls	*P* Values
R frontal horn	4.4 ± 0.8	3.2 ± 0.2	.21
L frontal horn	4.5 ± 0.6	2.7 ± 0.1	.15
R occipital horn	9 ± 0.9	7.9 ± 0.4	.15
L occipital horn	8,7 ± 0.8	8.2 ± 0.4	.8
Third ventricle	5.1 ± 1.8	3.4 ± 0.3	.73

Note:—R indicates right; L, left.

were statistically significant in LI (Tables 2 and 3). Cerebral atrophy appeared during the follow-up in 2/5 LI patients (mean age, 4 years; mean duration of disease, 2 years 9 months) and in 2/3 EJ patients (mean age, 8 years 2 months; mean duration of disease, 4 years 2 months).

Cerebellum. Vermian atrophy was present on the initial MRI in 3/10 LI patients (mean age, 2 years 7 months; mean duration of disease, 1 year 4 months) and in all 3 of the EJ patients and was found together with cerebellar WM hyperintensity in only 3 cases (2/10 LI, 1/3 EJ) and with cerebral atrophy in only 4 cases (3/10 LI, 1/3 EJ). It was found alone, without cerebral atrophy or cerebellar WM hyperintensity, in 2/3 EJ patients. Vermian atrophy developed subse-

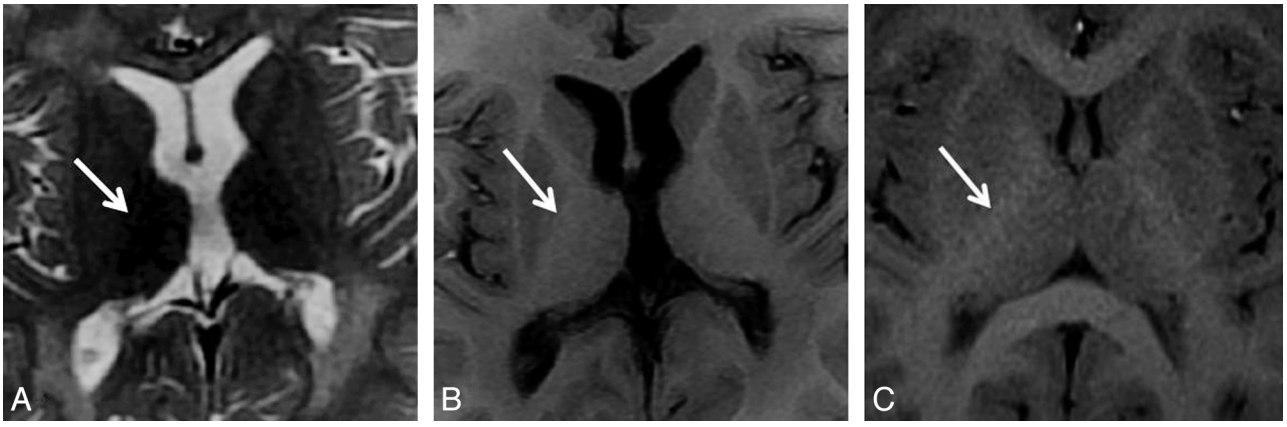

Fig 5. LI (3 years 11 months). *A,* Axial T2-weighted image shows the absence of frank T2 hyperintensity in the posterior limb of the internal capsule (*arrow*). *B,* Axial T1-weighted image shows loss of differentiation between the capsule and thalamus (*arrow*). *C,* Age-matched control. Image shows good differentiation between the capsule and thalamus (*arrow*).

quently in 2/5 LI patients without initial cerebellar abnormality (mean age, 5 years 2 months; mean duration of disease, 2 years 10 months), in both cases accompanied by cerebral atrophy. It was always associated with an MRI score of >18. There was a statistically significant fourth ventricle enlargement compared with the controls (6% for LI patients and 32% for EJ patients, $P < .05$).

Deep Gray Nuclei. A loss of contrast between the posterior limb of the internal capsule and the thalamus was noticed in all patients (10/10 LI, 3/3 EJ)—including those without internal capsule T2 hyperintensity—and was seen on the T1-weighted images compared with those of controls (Fig 5). This pattern was present since the initial MRI and remained stable during the follow-up.

The thalami on initial T2-weighted images had abnormal low signal intensity in 9/10 LI patients and all of the EJ patients, and the abnormal low signal intensity developed in the course of follow-up in the only LI patient without initial involvement (duration of disease, 1 year 9 months). Thalamic atrophy was significant ($P < .05$) (Table 4) only in EJ patients (Fig 6). Although no caudate signal-intensity abnormalities were seen, a statistically significant atrophy ($P < .05$) was measured initially in 2/3 EJ patients and developed in 1/3 EJ patients (mean duration of disease, 5 years 4 months) (Table 4). Caudate nucleus size was correlated with thalamus size (Fig 7). None of the LI or EJ patients had lenticular nucleus involvement.

Table 4: Mean values of measures of thalami and caudate nuclei (length, width, curve, and surface) compared with controls at the same age, with corresponding *P* values

	Values (mean ± SE) (mm)		
Measures	EJ	Controls	*P* Values
Length of R thalamus	27.3 ± 0.7	32.6 ± 0.4	<.0001
Length of L thalamus	27.7 ± 0.6	32.4 ± 0.4	<.0001
Width of R thalamus	11.3 ± 0.3	15.2 ± 0.3	<.0001
Width of L thalamus	12.3 ± 0.7	15.1 ± 0.2	<.0001
Curve of R thalamus	68.3 ± 1.4	82.2 ± 0.7	<.0001
Curve of L thalamus	68.3 ± 1.4	83.6 ± 0.4	<.0001
Surface of R thalamus	263.6 ± 7.6	444.7 ± 2.8	<.0001
Surface of L thalamus	267.3 ± 5.5	442.5 ± 3	<.0001
Length of R caudate nucleus	15.3 ± 0.3	18.4 ± 0.2	<.0001
Length of L caudate nucleus	15.6 ± 0.3	18.6 ± 0.3	<.0001
Width of R caudate nucleus	7 ± 0.5	8.3 ± 0.2	<.0001
Width of L caudate nucleus	6.6 ± 0.6	8.1 ± 0.2	<.0001
Curve of R caudate nucleus	38 ± 1.3	44.5 ± 0.4	<.0001
Curve of L caudate nucleus	38 ± 1.3	44.9 ± 0.3	<.0001
Surface of R caudate nucleus	88.3 ± 2.9	120.9 ± 2	<.0001
Surface of L caudate nucleus	88.3 ± 2.9	117.9 ± 1.8	<.0001

Note:—R indicates right; L, left.

DWI Patterns

Nine (7/10 LI, 2/3 EJ) of the 13 patients had an initial DWI sequence, and 6 (4/10 LI, 2/3 EJ) had DWI follow-up. One of 2 EJ patients (age, 5 years) had a periventricular WM high signal intensity on the initial $b = 1000$ DWI, with an 0.8-fold reduction in ADC.[11] Six patients (1/2 EJ, 5/7 LI) had hyperintensity in the CC on the initial $b = 1000$ DWI; it was in the splenium in 4 cases (1/1 EJ, 3/5 LI) and in both the genu and splenium in 2/5 LI cases. CC hyperintensity developed during follow-up in the splenium in 1/4 LI patients (duration of disease, 1 year 10 months) and in the splenium and then the genu in 1/4 LI patients (duration of disease, 2 years 6 months) and 1/2 EJ patients. In all cases, the ADC was reduced when the signal intensity was high (by 6% in the splenium and 14% in the genu), with variable change during the course of follow-up. There was a reduction in the ADC in the genu and splenium for 1/2 EJ patients and an increase in the ADC for the other EJ patient. There were 2/4 LI patients with a reduction in the ADC in the splenium and no change in the genu. One LI patient showed increased splenium ADC and decreased genu ADC. Moreover, finally, 1 LI patient had no abnormality, either initially or in the course of follow-up. No DWI abnormalities were seen in the thalami, caudate nuclei, or lenticular nuclei in the $b = 1000$ sequence.

MR Spectroscopy

MR spectroscopy was available for 8/10 LI and 3/3 EJ patients. There was a reduced NAA/Cr ratio in 7/8 LI patients (mean score, 19) and 1/3 EJ patients (score, 18); an elevated Cho/Cr ratio in 7/8 LI (mean score, 19) and 1/3 EJ patients (score, 18); a lactate resonance in 4/8 LI (mean score, 20) and 1/3 EJ patients (MRI score, 24); and an elevated myo-inositol level in 3/8 LI (mean MRI score, 21) and 2/3 EJ patients (mean MRI

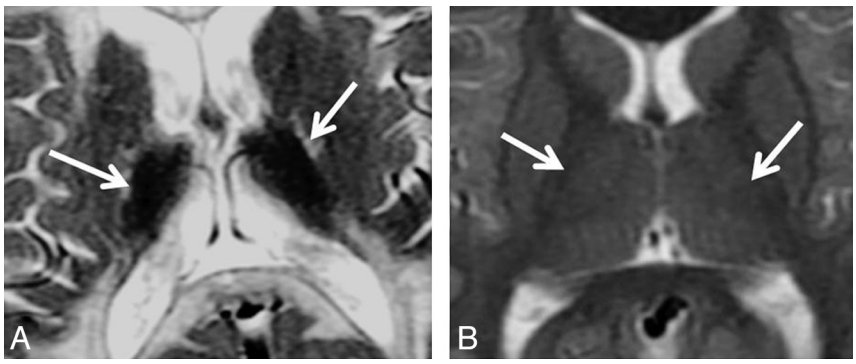

Fig 6. Axial T2-weighted sequences. *A,* EJ (5 years of age). Note frank T2 hypointensity and atrophy of the thalami (*arrows*). *B,* Age-matched control. Note the normal appearance of the thalami (*arrows*).

Fig 7. *A,* Axial T2-weighted sequence. LI (3 years 7 months of age). Note atrophy of the caudate nuclei and thalami and lack of significant decrease in the volume of the putamina. *B,* Age-matched control. Note the normal appearance of the caudate nuclei (*arrows*) and thalami. *C,* Correlation between the length of the thalami (T) and the caudate nuclei (CN) in EJ patients ($r = 0.8$, $P = .0002$).

Table 5: Spectroscopy at first MRI[a]

Patient	Sex	Score	Age (yr/mo) (MRI)	Time to Onset of Clinical Symptoms (yr)	NAA Decreased	Cho Increased	Lactate Resonance	Myo-Inositol Increased
LI								
1	F	19	2.12	1.02				
2	M	19	3.08	1.66	1	1	1	0
3	M	14	2.66	1.66	1	1	0	0
4	M	24	2.42	1.6	0	0	0	0
5	M	21	2.83	1.33	1	1	1	1
6	M	12	3.33	1.83	0	0	0	0
		17	4	3.5	1	1	1	1
7	M	23	2.75	1.09	1	1	1	1
8	M	17	3.9	2.5	1	1	0	0
EJ								
9	F	24	4.5	0.67	0	0	1	1
10	F	25	6.16	3	0	0	0	0
11	F	18	5.4	1.25	1	1	0	1

[a] 0 = absent, 1 = present.

score, 21). The most common profile among the LI patients was thus reduced NAA and an elevated Cho/Cr ratio, whereas among the EJ patients, elevated myo-inositol was more common (Table 5). Only 1 patient (LI) had another MR spectroscopy in the course of follow-up, and this showed the onset of decreased NAA, an increased Cho/Cr ratio, and a lactate resonance (4 years of age).

Discussion

MLD is a rare lysosomal storage disorder, more often due to a deficit in ARSA enzyme activity than to a Saposin B deficiency. It results in central and peripheral nervous system demyelination, due to an inability to break down sulfatides—in particular, 3-O-sulfogalactosylceramide, a major constituent of the myelin sheath. Damage to CNS myelin can be visualized on MRI and is classically described as bilateral symmetric confluent sheets of high T2 signal intensity in the periventricular WM, which extends to the semiovale centers and spares the subcortical U fibers.[12,13] A scoring system, recently developed by Eichler et al,[5] based on the scoring system for adrenoleukodystrophy,[14] should be a valuable tool for evaluating the response to treatment.

Several stages were defined, with a maximum score of 34: mild disease, 1–6; moderate disease, 7–15; and severe disease, 16–34. In our series, we found some interesting potential differences between LI and EJ forms, though those may just represent different stages/severity of the disease related to the underlying biochemical phenotype differences. However, the residual enzymatic activity, as routinely tested, resulted in extreme variability and did not correlate with clinical onset and evolution, especially in early-onset forms of the disease.

The high T2 signal intensity in the WM, graded according to the scoring system of Eichler et al[5] (faint or attenuated), is barely visible initially only on images of some LI patients. More recently, a tigroid pattern within a hyperintense area has been reported, not just as a diagnostic sign but as an indication of advanced disease.[5] Our study confirms this finding, because the tigroid appearance—which is more easily visualized on T2-weighted than on FLAIR images[13]—was always associated with a severity score of ≥13 (moderate disease) and was found in all of the EJ patients and in only 60% of LI patients. The T2 hyperintensity of the corticospinal tracts—present in the pons and in the posterior limbs of the internal capsule—is uniformly associated with an advanced disease and thus is more often seen in EJ forms.

Some patients in our study showed a diffusion restriction in the splenium of the CC that may represent an ARSA deficiency–related accumulation of macromolecules (sulfatides) within the oligodendrocytes[11] or myelin edema rather than cytotoxic edema.[12,15,16]

The MR spectroscopic findings in our series differed depending on the clinical form of MLD; while reduced NAA and elevated Cho/Cr ratio were more common in the LI, elevated myo-inositol predominated in the EJ. The MR spectroscopic profile of MLD is well-known[17]; for short TEs (20–40 ms), there is a reduction in the NAA peak, reflecting neuronal distress, along with a significant increase in the myo-inositol peak, which may correspond to either galactosylceramide accumulation or secondary glial activation. The study by Dali et al[18] suggests that the NAA level may be a sensitive disease marker, correlated to clinical motor and cognitive function performance, which can be used to assess treatment efficacy. The lactate resonance described[19] may correspond to anaerobic metabolism from myelin destruction and the elevation in Cho to cell membrane degradation (due to the accumulation of sulfatides). There are few correlations in the literature between abnormal Cho/Cr ratios and MRI severity scores. In our study, the increased Cho/Cr ratio and decreased NAA are associated with a mean score of >18 and elevated myo-inositol and a lactate resonance with a mean score >20.

Eight patients had follow-up MRI during a maximum period of 5 years 5 months. To the best of our knowledge, this is longer than the data available in the literature[5] and offers a better understanding of the natural history of this rare disease. Most interesting, some differences in lesion progression between LI and EJ do exist. Very significant disease progression can be seen in the LI patients (mean initial score, 8.8; mean follow-up score, 15.5; mean follow-up period, 1 year) and, to a lesser extent (<2 points), in the EJ patients (mean initial score, 22; mean follow-up score, 23.7; mean follow-up period, 2 years 8 months). We found marked classic topographic changes, with occipitofrontal progression, extension of abnormal WM to the semiovale centers, and onset of a tigroid pattern,[13] only in LI patients, while disease in all of the EJ patients was stable. Like Eichler et al,[5] we also noted an increase in signal intensity with time, appreciated subjectively on the FLAIR and T2-weighted sequences. Cerebral atrophy appeared earlier in LI than in EJ.

Some specific patterns can be detailed, and it might be interesting to focus on the time of their occurrence in the course of the disease and their relationship to the score of Eichler et al. As in the literature,[1,13] the CC was involved in all patients from the initial diagnostic MRI. In our series, however, CC involvement differed depending on the disease stage, and we need to be aware of the patterns of progression, to avoid pitfalls in scoring. Those changes seem to start centrally and then become "diffuse," and they ultimately become "curvilinear." This may be true for both the splenium and the genu, except that there is a time shift between the 2 regions reflecting the posteroanterior progression trend of the WM changes. Hence, central hyperintensity of the genu or diffuse hyperintensity of the splenium or both may indicate moderate severity scores (mean score, 13). Conversely, diffuse genu involvement and curvilinear splenium involvement may be indicative of high severity scores (mean score, 17).

In our series, CC atrophy was present at initial MRI in all of the EJ patients (splenium, $P < .05$). It seems to be one of the markers for severe disease (mean score, >18). This is comparable with what is seen in acquired diseases such as periventricular leukomalacia and multiple sclerosis, where several studies[20-22] point to a correlation between CC atrophy and WM volume, suggesting that the thickness of the middle part of the CC could be used as an indicator of WM loss.

Cerebellar involvement deserves particular attention. Similar to that in previous studies,[1,5,13] T2 hyperintensity in the cerebellar WM occurred at advanced stages of the disease. Most interesting, this vermian atrophy appeared indeed "isolated" (ie, without cerebellar WM involvement and global cerebral atrophy) in 2 of the EJ patients in our series—something not previously reported and possibly underestimated. This early cerebellar atrophy may reflect a primary involvement of the cerebellar cortex itself, thus supporting the possibility of granular layer involvement.[6] MLD is usually considered a storage disease involving primarily oligodendrocytes, resulting in demyelination. However, several elements argue for an associated neuronal disease.[7,8] As a consequence, MLD mice display a significant loss of Purkinje cells and degeneration of the acoustic ganglions and cochlear nuclei.[7,8] In patients with MLD, cerebral atrophy already found at an early stage of the disease may also reflect neuronal loss. Last, patients with late-onset forms of MLD may have psychiatric or schizophrenia-like symptoms as the initial manifestation before neurologic symptoms occur, suggesting neuronal dysfunction.

We initially found a hypointense thalamic T2 signal intensity in 92% (only 1 LI patient was spared initially, but involved secondarily)—a much higher percentage than that reported in the literature.[12,13] In our series, the low T2 signal intensity corresponded to high signal intensity on the T1-weighted sequences, which may explain the loss of capsule-thalamus contrast seen on the T1-weighted images in all of our patients

since their initial MRI. We have not seen this finding reported in any earlier studies. A review of the literature[23] on lysosomal storage diseases attributes thalamic T2 hypointensity to an accumulation of paramagnetic substances such as iron, free radicals, and deoxygenated hemoglobin. This explanation is controversial, however; the phenomenon is more likely related to changes in tissue viscosity due to an accumulation of macromolecules and lipids.[24] Therefore, the main hypotheses to explain the thalamic T2 hypointensity in MLD are sulfatide deposits that alter the viscosity and an accumulation of iron. It is also interesting to compare this with the low thalamic T2 signal intensity observed in multiple sclerosis,[25] for which several hypotheses have been proposed, including hypometabolism of iron, a breakdown in the blood-brain barrier, and an increase in free radical levels causing membrane peroxidation and thus iron deposition. The hypointensity is reported to be directly correlated with WM involvement, cerebral atrophy, and the degree of clinical disability.[26-29] Associated with the signal-intensity abnormalities, significant thalamic atrophy ($P < .05$) was noted by us for all early juvenile forms. Because this thalamic atrophy is associated with MRI scores of >14, indicating moderate disease, it may imply a primary neuronal dysfunction despite the presence of myelination within the thalami. There was no correlation between the MRI severity score and thalamic size, and we did not find any correlation between thalamic atrophy and third ventricle enlargement.[30,31] A recent study found a correlation between thalamic and CC atrophy and the severity of cognitive impairment in children with multiple sclerosis.[32]

Friede[6] described supra- and infratentorial GM involvement as rare or nonexistent and regionally selective, with metachromatic deposits within the thalamus, the globus pallidus, and the dentate nucleus, but sparing the caudate nucleus and putamen. Nevertheless, in our series, caudate atrophy ($P < .05$) was always found together with thalamic atrophy and with MRI scores of >19. This has not been reported previously, to the best of our knowledge, and might correspond to secondary GM lesions rather than primary lesions because caudate atrophy appears secondary to thalamic atrophy. While we were able to establish a parallel between the enlargement (primarily) of the frontal horns and the stage of cerebral atrophy, we were unable to demonstrate a correlation with the size of the caudate nuclei, perhaps due to a lack of statistical power. The cortex, thalamus, and basal ganglia are closely interrelated via numerous connections (cortico-striato-pallido-thalamo-cortical pathways). A recent article by Smith et al[33] examined the correlations between the location of MRI WM lesions, executive function, and episodic memory (in patients with no cognitive impairment and at various stages of dementia) and concluded that WM hyperintensities may be responsible for cognitive impairment by interfering with the connections between the cortex, thalamus, and striatum.

Should we, at this point, consider adding some new items to the scoring method of Eichler et al to increase its sensitivity, particularly for mild and moderate forms? While the loss of capsule-thalamus contrast seen on the T1-weighted images does not seem to have any value in discriminating the severity of the disease—because it can be found at any stage and in any form of the disease—central genu hyperintensity, a tigroid pattern, and thalamic atrophy could be used as markers of moderate disease. In contrast, curvilinear signal-intensity hyperintensity in the splenium, semiovale involvement, and CC and caudate nucleus atrophy are markers of severe disease, and a decrease in diffuse signal-intensity hyperintensity in the CC should not be mistaken for disease regression.[32]

Certain limitations of this study should, however, be noted. Because the study is retrospective, there may be some variability in the MRI technique, though this might have been mitigated, in part, by the use of a standardized leukodystrophy protocol. Moreover, the small sample size—readily explained by the rarity of the disorder—limits its statistical power. Another limitation is that DWI and ADC values were not available for our own control population.

Conclusions

This analysis of MRI changes adds to our understanding of the natural history of MLD. In addition to the classic MLD data—which basically describe the WM—thalamic changes may be common and primary in MLD, and isolated cerebellar atrophy may be observed in some peculiar later onset forms. Such patterns raise the question of primary GM injury, and thus the possibility of neuronal involvement in MLD. These data become especially important in light of the new treatment modalities, such as gene therapy, because very precise imaging follow-up will be needed to assess their efficacy.

Disclosures: Patrick Aubourg—*UNRELATED: Employment:* Assistance Publique des Hôpitaux de Paris and University Paris Descartes, *Comments:* As professor of pediatrics, half of my salary comes from Assistance Publique-Hôpitaux de Paris (for the clinical work I perform) and the other half from the University Paris-Descartes (research and teaching), *Grants/Grants Pending:* French Agence Nationale de la Recherche European,* European Framework Program,* Association France-Alzheimer,* Association Europeenne contre les Leucodystrophies.* Catherine Adamsbaum—*UNRELATED: Expert Testimony:* Judicial Expert in Pediatric Radiology approved by the French Courts (Paris and Cassation, public service). *Money paid to the institution.

References

1. Cheon JE, Kim IO, Hwang YS, et al. **Leukodystrophy in children: a pictorial review of MR imaging features.** *Radiographics* 2002;22:461–76
2. Fluharty AL. **Arylsulfatase A deficiency.** *Gene Reviews 2006*. [Internet]. Seattle: University of Washington, Seattle; 1993–2006 May 30 [updated 2011 Aug 25]
3. Demaerel P, Faubert C, Wilms G, et al. **MR findings in leukodystrophy.** *Neuroradiology* 1991;33:368–71
4. Cartier N, Aubourg P. **Hematopoietic stem cell transplantation and hematopoietic stem cell gene therapy in X-linked adrenoleukodystrophy.** *Brain Pathol* 2010;20:857–62
5. Eichler F, Grodd W, Grant E, et al. **Metachromatic leukodystrophy: a scoring system for brain MR imaging observations.** *AJNR Am J Neuroradiol* 2009;30:1893–97
6. Friede RL, ed. *Developmental Neuropathology.* Berlin: Springer-Verlag; 1989:461–469
7. Molander-Melin M, Pernber Z, Franken S, et al. **Accumulation of sulfatide in neuronal and glial cells of arylsulfatase A deficient mice.** *J Neurocytol* 2004;33:417–27
8. Wittke D, Hartmann D, Gieselmann V, et al. **Lysosomal sulfatide storage in the brain of arylsulfatase A-deficient mice: cellular alterations and topographic distribution.** *Acta Neuropathol* 2004;108:261–71. Epub 2004 Aug 20
9. Barkovich AJ, Kjos BO. **Normal postnatal development of the corpus callosum as demonstrated by MR imaging.** *AJNR Am J Neuroradiol* 1988;9:487–91
10. Rakic P, Yakovlev PI. **Development of the corpus callosum and cavum septi in man.** *J Comp Neurol* 1968;132:45–72
11. Engelbrecht V, Scherer A, Rassek M, et al. **Diffusion-weighted MR imaging in the brain in children: findings in the normal brain and in the brain with white matter diseases.** *Radiology* 2002;222:410–18
12. Sener RN. **Metachromatic leukodystrophy: diffusion MR imaging and proton MR spectroscopy.** *Acta Radiol* 2003;44:440–43
13. Kim TS, Kim IO, Kim WS, et al. **MR of childhood metachromatic leukodystrophy.** *AJNR Am J Neuroradiol* 1997;18:733–38
14. Loes DJ, Hite S, Moser H, et al. **Adrenoleukodystrophy: a scoring method for brain MR observations.** *AJNR Am J Neuroradiol* 1994;15:1761–66

15. Sener RN. **Metachromatic leukodystrophy: diffusion MR imaging findings.** *AJNR Am J Neuroradiol* 2002;23:1424–26
16. Patay Z. **Diffusion-weighted MR imaging in leukodystrophies.** *Eur Radiol* 2005;15:2284–303
17. Galanaud D, Aubourg P, Kalifa G, et al. **What is your diagnosis? Metachromatic leukodystrophy.** *J Neuroradiol* 2002;29:173–75
18. Dali C, Hanson LG, Barton NW, et al. **Brain N-acetylaspartate levels correlate with motor function in metachromatic leukodystrophy.** *Neurology* 2010;75:1896–903
19. Kruse B, Hanefeld F, Christen HJ, et al. **Alterations of brain metabolites in metachromatic leukodystrophy as detected by localized proton magnetic resonance spectroscopy in vivo.** *J Neurol* 1993;241:68–74
20. Hayakawa K, Kanda T, Hashimoto K, et al. **MR imaging of spastic diplegia. The importance of corpus callosum.** *Acta Radiol* 1996;37:830–36
21. Iai M, Tanabe Y, Goto M, et al. **A comparative magnetic resonance imaging study of the corpus callosum in neurologically normal children and children with spastic diplegia.** *Acta Paediatr* 1994;83:1086–90
22. Panigrahy A, Barnes PD, Robertson RL, et al. **Quantitative analysis of the corpus callosum in children with cerebral palsy and developmental delay: correlation with cerebral white matter volume.** *Pediatr Radiol* 2005;35:1199–207
23. Autti T, Joensuu R, Aberg L. **Decreased T2 signal in the thalami may be a sign of lysosomal storage disease.** *Neuroradiology* 2007;49:571–78
24. Bloembergen N, Purcell EM, Pound RV. **Nuclear magnetic relaxation.** *Nature* 1947;160:475
25. Ge Y, Jensen JH, Lu H, et al. **Quantitative assessment of iron accumulation in the deep gray matter of multiple sclerosis by magnetic field correlation imaging.** *AJNR Am J Neuroradiol* 2007;28:1639–44
26. Neema M, Stankiewicz J, Arora A, et al. **T1- and T2-based MRI measures of diffuse gray matter and white matter damage in patients with multiple sclerosis.** *J Neuroimaging* 2007;17:16S–21S
27. Bakshi R, Dmochowski J, Shaikh ZA, et al. **Gray matter T2 hypointensity is related to plaques and atrophy in the brains of multiple sclerosis patients.** *J Neurol Sci* 2001;185:19–26
28. Bakshi R, Benedict RH, Bermel RA, et al. **T2 hypointensity in the deep gray matter of patients with multiple sclerosis: a quantitative magnetic resonance imaging study.** *Arch Neurol* 2002;59:62–68
29. Bermel RA, Puli SR, Rudick RA, et al. **Prediction of longitudinal brain atrophy in multiple sclerosis by gray matter magnetic resonance imaging T2 hypointensity.** *Arch Neurol* 2005;62:1371–76
30. Houtchens MK, Benedict RH, Killiany R, et al. **Thalamic atrophy and cognition in multiple sclerosis.** *Neurology* 2007;69:1213–23
31. Mesaros S, Rocca MA, Absinta M, et al. **Evidence of thalamic gray matter loss in pediatric multiple sclerosis.** *Neurology* 2008;70:1107–12
32. Goodman A. **Reduced thalamic and corpus callosum areas found to correlate with cognitive impairment in childhood-onset MS.** *Neurology Today* 2010:10:6
33. Smith EE, Salat DH, Jeng J, et al. **Correlations between MRI white matter lesion location and executive function and episodic memory.** *Neurology* 2011;76:1492–99